BBA - Proteins and Proteomics 1870 (2022) 140797

Contents lists available at ScienceDirect

BBA - Proteins and Proteomics

journal homepage: www.elsevier.com/locate/bbapap

Research paper

Protein oxidation marker, α-amino adipic acid, impairs proteome of differentiated human enterocytes: Underlying toxicological mechanisms

S. Díaz-Velasco [a], J. Delgado [b], F.J. Peña [c], Mario Estévez [a,*]

[a] Food Technology and Quality (TECAL), Institute of Meat and Meat Products (IPROCAR), Universidad de Extremadura, Cáceres, Spain
[b] Food Hygiene and Safety (HISEALI), Institute of Meat and Meat Products (IPROCAR), Universidad de Extremadura, Cáceres, Spain
[c] Spermatology Laboratory, Universidad de Extremadura, Cáceres, Spain

ARTICLE INFO

Keywords:
α-Amino Adipic acid
Mitochondria
Na^+/K^+-ATPase
Tricarboxylic acid cycle
Proteomics
Flow cytometry

ABSTRACT

Protein oxidation and oxidative stress are involved in a variety of health disorders such as colorectal adenomas, inflammatory bowel's disease, neurological disorders and aging, among others. In particular, the specific final oxidation product from lysine, the α-amino adipic acid (α-AA), has been found in processed meat products and emphasized as a reliable marker of type II diabetes and obesity. Currently, the underlying mechanisms of the biological impairments caused by α-AA are unknown. To elucidate the molecular basis of the toxicological effect of α-AA, differentiated human enterocytes were exposed to dietary concentrations of α-AA (200 μM) and analyzed by flow cytometry, protein oxidation and proteomics using a Nanoliquid Chromatography-Orbitrap MS/MS. Cell viability was significantly affected by α-AA ($p < 0.05$). The proteomic study revealed that α-AA was able to alter cell homeostasis through impairment of the Na^+/K^+-ATPase pump, energetic metabolism, and antioxidant response, among other biological processes. These results show the importance of dietary oxidized amino acids in intestinal cell physiology and open the door to further studies to reveal the impact of protein oxidation products in pathological conditions.

1. Introduction

Oxidative stress and protein oxidation are involved in assorted health disorders such as cardiovascular disease, neurological disorders, diabetes, aging, rheumatoid arthritis, muscular dystrophy, Parkinson's syndrome and Alzheimer's disease [1,2]. Other pathological conditions such as inflammatory bowel's disease (IBD) [3] and colorectal adenomas [4] are closely related to oxidative stress and chronic inflammation. The accretion of oxidized proteins as a result of enduring oxidative stress impairs cellular homeostasis and leads to physiological impairments [1]. Furthermore, oxidized proteins and amino acids are markers of several of the aforementioned diseases. In particular, the α-amino adipic acid (α-AA), the specific final oxidation product of lysine, has been emphasized as a reliable marker of cataractogenesis, renal failure and aging [5], and more recently as an early indicator of type II diabetes and obesity [6,7]. Even though the ability of α-AA to impair both endocrine and exocrine pancreas physiology has been documented, the underlying molecular mechanisms of the toxic effects of specific oxidized amino acids, such as α-AA, in human cells, is mostly unknown. Estaras et al. [8] reported that α-AA has deleterious actions on mouse pancreatic acinar cells. Moreover, α-AA is associated with disorders in brain and pancreatic tissues [9]. According to da Silva et al. [10] α-AA caused oxidative stress in neuronal cells of rats, which led to pathophysiological alterations in nervous tissue. In a previous in vitro study on differentiated human colon CACO-2 cell line [11], we reported that α-AA caused a ROS-mediated cytotoxic effect, leading to apoptotic events. These results are relevant since dietary oxidized proteins and α-AA have been found to contribute to in vivo oxidative stress and cause toxicological effects on intestinal cells and on internal organs, upon intestinal uptake [6,12]. α-AA has been found in concentrations up to 200 μM in severely processed meat products such as ready-to-eat beef patties [13]. Interestingly, processed meat and red meat were included in 2015 by the International Agency for Research on Cancer [14] in groups 1 and 2A of carcinogenic substances, based on epidemiological studies. Yet again, the potential implication of dietary oxidized amino acids on this and many other pathological conditions linked to oxidative stress, is unknown.

The present study aims to decipher the molecular basis of the toxicological effect of α-AA on differentiated human colon CACO-2 cells. To fulfil this objective, these intestinal cells were exposed to dietary

* Corresponding author at: Institute of Meat and Meat Products (IPROCAR), University of Extremadura, Avd. Universidad, sn. 10003 Cáceres, Spain.
E-mail address: mariovet@unex.es (M. Estévez).

https://doi.org/10.1016/j.bbapap.2022.140797
Received 5 April 2022; Received in revised form 28 May 2022; Accepted 6 June 2022
Available online 9 June 2022

concentrations of α-AA (200 μM) and subsequently analyzed by means of a high-resolution mass spectrometry-based proteomics using a Nanoliquid Chromatography-Orbitrap MS/MS. CACO-2 cells are used as an experimental model since their spontaneous differentiation for 21 days allows them to achieve morphological and biochemical characteristics similar to enterocytes [15]. Supportive flow cytometry studies and protein oxidation measurements were applied.

2. Material and methods

2.1. Chemicals

All reagents, chemicals and α-AA standard compound (CAS Number 542–32-5) were obtained from Sigma Chemicals (Sigma-Aldrich, Steinheim, Germany), Fisher (Fisher Scientific S.L., Madrid, Spain) and Panreac (Panreac Química, S. A., Barcelona, Spain). Ultrapure water was prepared by Milli-Q water purification system (Millipore Corp, Bedford, MA).

2.2. Cell culture

Human colon adenocarcinoma CACO-2 cell line was purchased from ECACC (European Collection of Authenticated Cell Cultures, Salisbury, UK). Passages between 40 and 46 were used for cell culture studies. Cells were grown in T-75 flasks in EMEM (Eagle's Minimum Essential Medium) supplemented with fetal bovine serum (FBS) (10% *v*/v), L-glutamine (1% v/v) and non-essential amino acids (1% v/v) at 37 °C in humidified atmosphere and 5% CO_2. When cells reached 90% confluence, they were allowed to differentiate into enterocytes for 21 days. Such differentiation was confirmed by visualization by phase-contrast microscopy. After that, they were harvested using 0.25% trypsin in 1 mM EDTA solution.

2.3. Experimental setting

α-AA was used at 200 μM and dissolved in 10 mL of supplemented EMEM. Concentrations of α-AA are food-compatible according to the data available in the literature [13,16–18]. α-AA was then added and exposed to enterocytes for 72 h in T-75 flasks at 37 °C in a humidified incubator 5%CO_2/95% air. For comparison purposes, CONTROL cells were incubated in standard EMEM in the same conditions. The whole experiment was replicated five times independent flasks for both treated and CONTROL cells. At 72 h, cells were harvested using 0.25% trypsin in 1 mM EDTA, centrifuged at 126*g* for 5 min and suspended in 1 mL of phosphate-buffered saline (PBS) solution for further analysis.

2.4. Flow cytometry analysis

Samples were diluted in PBS to a final concentration 5×10^6 cells/mL and analyses were carried out using a Cytoflex® LX flow cytometer (Beckman Coulter, Brea, CA, USA) equipped with blue, red, violet, ultraviolet, yellow and infrared lasers. The instrument was calibrated daily employing specific calibration beads provided by the manufacturer. A compensation overlap was performed before each experiment. Files were exported as FCS files and loaded and analyzed using Cytobank Software (Beckman Coulter, Brea, CA, USA). Cells were stained with 1 μL of Hoechst 33342 (16.2 mM stock solution), 1 μL of CellROX Deep Red ® (2.5 mM stock solution), and 0.3 μL of JC-1 (1 μM) to measure cell viability, ROS occurrence and mitochondrial activity, respectively. After thorough mixing, the cell suspension was incubated at room temperature in the dark for 20 min; then 10 μM of MCB-1 were added to the samples and incubated for a further 10 min to measure the reduced form of glutathione (GSH) concentration. Dead cells were excluded after staining the cells with ViaKrome 808 Fixable Viability Dye (Beckman Brea, CA, USA) following the instructions of the manufacturer. Lastly, the samples were filtered through MACS® smart trainer 30 μm filters and immediately run on the flow cytometer. Hoechst 33342 was excited with the violet laser (355 nm) and fluorescence recorded at 450/50 nm band pass filter; MCB was excited with the violet laser (405 nm) and fluorescence recorded at 405/30 bandpass filter, JC-1 was excited with the yellow laser (561 nm) the aggregates and blue laser (488 nm) the monomers and fluorescence collected at 525/50 and 610/20 nm bandpass filters respectively; CellROX® deep red was excited with the red laser 638 nm and fluorescence collected at 660/10 nm bandpass, finally, Viakrome 808 was excited with the infrared laser (808 nm) and fluorescence collected at 885/40 nm bandpass filter. The controls consisted of unstained and single-stained controls to properly set gates and compensations. Positive controls for high mitochondrial membrane potential (JC-1) consisted in high-quality stallion spermatozoa, these cells present a high mitochondrial activity [19]. Positive controls for reactive oxygen species (ROS) consisted of cells treated with menadione as indicated in Muñoz et al. [20].

2.5. Analysis of protein oxidation markers

Two main protein carbonyls, the α-aminoadipic and γ-glutamic semialdehydes (α-AS and γ-GS, respectively) were quantified in the enterocytes from the present study. The procedure described by Utrera et al. was followed with minor modifications [21]. One hundred μL of the cell lysates were dispensed in 2 mL screw-capped Eppendorf tubes and treated with 1 mL of cold 10% trichloroacetic acid (TCA) solution. Each Eppendorf was vortexed and then proteins were precipitated with centrifugation at 2240*g* for 5 min at 4 °C. The supernatant was removed, and the resulting pellet was treated again with 1 mL of cold 5% TCA solution. A new centrifugation was performed at 2240*g* for 5 min at 4 °C for protein precipitation. The supernatant was removed, and then the pellets were derivatized with p-amino-benzoic acid (ABA), purified and hydrolyzed following the procedure described elsewhere [21]. The hydrolysates were evaporated at 40 °C in vacuo to dryness using a centrifuge concentrator (Eppendorf, Hamburg, Germany). Finally, the generated residue was reconstituted with 200 μL of Milli-Q water and then filtered through hydrophilic polypropylene GH Polypro (GHP) syringe filters (0.45 μm pore size, Pall Corporation, NJ, USA) for HPLC analysis. Details on the chromatograph apparatus as well as on the separation, elution and identification of the compounds of interest were published elsewhere [21]. α-AS-ABA and γ-GS-ABA were synthesized and purified following the procedure reported by Akagawa et al. [22] and injected in the same conditions than samples. Both semialdehydes were identified in samples by comparing their retention times with those of the reference pure compounds. Standard solutions of ABA (ranging from 0.1 to 0.5 mM) were also injected in the same chromatographic conditions to create a standard curve. The peaks corresponding to both semialdehydes were manually integrated and the resulting areas plotted against the aforementioned standard curve. Results are expressed as nmol of protein carbonyl per mg of protein.

2.6. Sample preparation for LC-MS/MS based proteomics

Samples were added 0.5 mL of lysis buffer pH 7,5 (100 mM Tris-HCl, 50 mM NaCl, 10% glycerol, 0.5 M EDTA pH 8,5). Immediately before use, lysis buffer was added 100 mM PMSF (Phenylmethansulfonylfluorid) and 100 μg/mL Pepstatin in a 1:100 proportion. Samples were shaken for a minute in an agitator adding to each screw-capped Eppendorf tube 3–4 magnetized metal balls at 30 1/s (Retsch, Haan, Germany). Then, they were sonicated 3 times in batches of 10 pulses (Branson Ultrasonics, Danbury, USA). Lysates were incubated on ice for 1 h and were centrifuged in a 5427 R (Eppendorf, Hamburg, Germany) at 18064*g* for 10 min at 4 °C. All the supernatant was passed into new screw-capped Eppendorf tubes. Protein concentration was measured with a Coomasie Protein Assay Reagent Ready to Use employing a Nanodrop 2000c Spectophotometer and a Nanodrop 2000 software (USA). Protein concentration must be ≥1 μg/μL. Aliquots

containing 50 μg of proteins were partially run in SDS-PAGE (4% stacking and 12% separating), just stopped when they reached the separating part of the gel to be in gel digested according to Shevchenko et al. [23], with some modifications. The gel was stained with Coomassie blue R250. Each lane was cut into 1 mm^3 pieces and then were subjected to in-gel digestion. Milli-Q water was added to each sample to wash them and were unstained with 100% methanol and 50 mM ammonium bicarbonate. After, samples were dehydrated for 5 min with 100% acetonitrile and 50 mM ammonium bicarbonate. Supernatant was removed and 100% acetonitrile was added. Then, supernatant was discarded and was dried at room temperature in vacuo using a centrifugal vacuum concentrator (Gyrozen, Daejeon, Korea). Samples were incubated with 0.5 M DTT in 50 mM ammonium bicarbonate for 20 min at 56 °C for protein reduction. The resulting free thiol (-SH) groups were alkylated by incubating the samples with 0.55 M iodoacetamide in 50 mM ammonium bicarbonate for 15 min at room temperature in the dark. Supernatant was removed and milli-Q water was added twice to wash samples and then were dehydrated for 5 min with 100% acetonitrile and 50 mM ammonium bicarbonate. Supernatant was removed and 100% acetonitrile was added, then it was discarded and dried in a vacuum concentrator. Samples were rehydrated with a mix of 50 mM ammonium bicarbonate, 1 μL of ProteaseMAX (Promega, USA) and 1.8 μg of trypsin (Promega). After, they were incubated for 1 h at 50 °C and added 1 μL of 100% formic acid to stop the proteolysis and were sonicated in a water bath for 5 min. Supernatant was removed of each sample and placed it into new screw-capped Eppendorf tubes for drying in a vacuum concentrator. Before analyzing the samples on the Orbitrap LC-MS/MS, loading buffer was added (98% milli-Q water, 2% acetonitrile, 0.05% trifluoroacetic acid), and sonicated in a water bath for 5 min and centrifuged at 18064*g* for 15 min at room temperature and put them into vials of Orbitrap LC-MS/MS.

2.7. Label-free quantitative proteomic analyses

A Q-Exactive Plus mass spectrometer coupled to a Dionex Ultimate 3000 RSLCnano (Thermo Scientific) analyzed 5 μg from each digest. Data was collected using a Top15 method for MS/MS scans [24]. Comparative proteome abundance and data analysis were carried out using MaxQuant software (version 1.6.0.15.0; https://www.maxquant.org/download_asset/maxquant/latest)) and Perseus (v 1.6.14.0) to organize the data and perform statistical analysis. Carbamidomethylation of cysteines was set as a fixed modification; oxidation of methionines and acetylation of N-terminals were set as variable modifications. Database searching was performed against *Homo sapiens* protein database (www.uniprot.org). The maximum peptide / protein false discovery rates (FDR) were set to 1% based on comparison to a reverse database. The LFQ algorithm was used to generate normalized spectral intensities and infer relative protein abundance. Proteins were identified with at least two peptides, and those proteins that matched to a contaminant database or the reverse database were removed, and proteins were only retained in final analysis if they were detected in at least two replicates from at least one treatment. Quantitative analysis was performed using a *t*-test to compare treatments with the control. The qualitative analysis was also performed to detect proteins that were found in at least three replicates of a given treated group but were undetectable in the comparison control group. All proteins satisfying one of these two aforementioned criteria were identified as discriminating proteins, and their corresponding genes were grouped by biological processes and molecular functions through ClueGO (v. 2.5.6) [25]. To define term-term interrelations and functional groups based on shared genes between the terms, the Kappa score was stablished at 0.4. Three GO terms and 4% of genes covered were set as the minimum required to be retained in the final result. The *p*-value was corrected by Bonferroni step down and set as $p \leq 0.05$.

2.8. Statistical analysis

All experiments were performed five times and each individual sample was analyzed twice for flow cytometry. Data was analyzed for normality and homoscedasticity. The effect of the exposure to α-AA was assessed by Analysis of Variance (ANOVA). The Tukey's test was used for multiple comparisons of the means. The effect of the incubation time on the same measurements was assessed by Student's *t*-test. The significance level was set at $p < 0.05$. SPSS (version 15.0) was used for statistical analysis of the data.

3. Results

3.1. Flow cytometry and protein oxidation markers

Parameters analyzed by flow cytometry were cell viability, mitochondrial activity, ROS occurrence, and reduced form of glutathione (GSH) concentration. Cells were processed and analyzed as described in material and methods. Fig. 1A-E show representative cytograms of the 6-colors experiment conducted as well as positive control for mitochondrial membrane potential and ROS production (Fig. 1F and G, respectively). Results show a significant decrease in viability among enterocytes exposed to α-AA compared to control cells ($p < 0.05$) (Fig. 1H). Cells exposed to α-AA showed a reduction in mitochondrial activity and an increase in ROS (Fig. 1I and J), though, in this case, not to a significant extent ($p > 0.05$). No significant differences were found between treatments for the concentration of GSH when considering live cells (data not shown). Yet, among the population of dead cells, a significant increase in GSH concentration was observed as compared to control counterparts (Fig. 1K).

The analysis of protein oxidation markers α-AS and γ-GS, revealed significantly higher concentrations of both protein carbonyls in cells exposed to α-AA (1.26 ± 0.31 nmol/mg protein; 0.49 ± 0.19 nmol/mg protein, respectively) than in the control cells (0.59 ± 0.11 nmol/mg protein; 0.21 ± 0.08 nmol/mg protein, respectively).

3.2. Proteomic analyses induced by α-AA

The LFQ analyses identified a total of 1695 proteins. Quantitative ($p < 0.05$) and qualitative (only detected in one condition) changes in protein abundance were identified (Table S1 Supplementary material). 234 proteins were significantly influenced by α-AA, among those, 91 were found in lower abundance in cells treated with α-AA while 45 were only found in control samples. Conversely, 97 proteins were detected in higher quantity by α-AA treatment and only one was found in α-AA-treated cells. For a rational and organized description and discussion of results, discriminating proteins and their corresponding genes were grouped by biological processes and molecular functions (Fig. 2A–D). Specific pathways for each of these processed and full details of identified proteins and associated genes are provided in Tables S2–S5 Supplementary material. Among all proteins identified in differentiated enterocytes, those which concentrations were more severely affected by the exposure to α-AA, are listed in Table 1. Only discriminating proteins having defined biological significance are presented in the following sections.

3.2.1. Proteins found in lower relative quantity in CACO-2 cells exposed to α-AA exposure

3.2.1.1. ATPase activity. The exposure to α-AA caused disturbance to a number of biological processes in enterocytes with Na^+/K^+-exchanging ATPase activity, being one the most affected among all biological processes (Fig. 2A and Supplementary Table S2) for the low abundance of the protein sodium/potassium-transporting ATPase subunit alpha-1 (ATP1A1; Fold change: 0.72) (Table 1 and Supplementary Table S1).

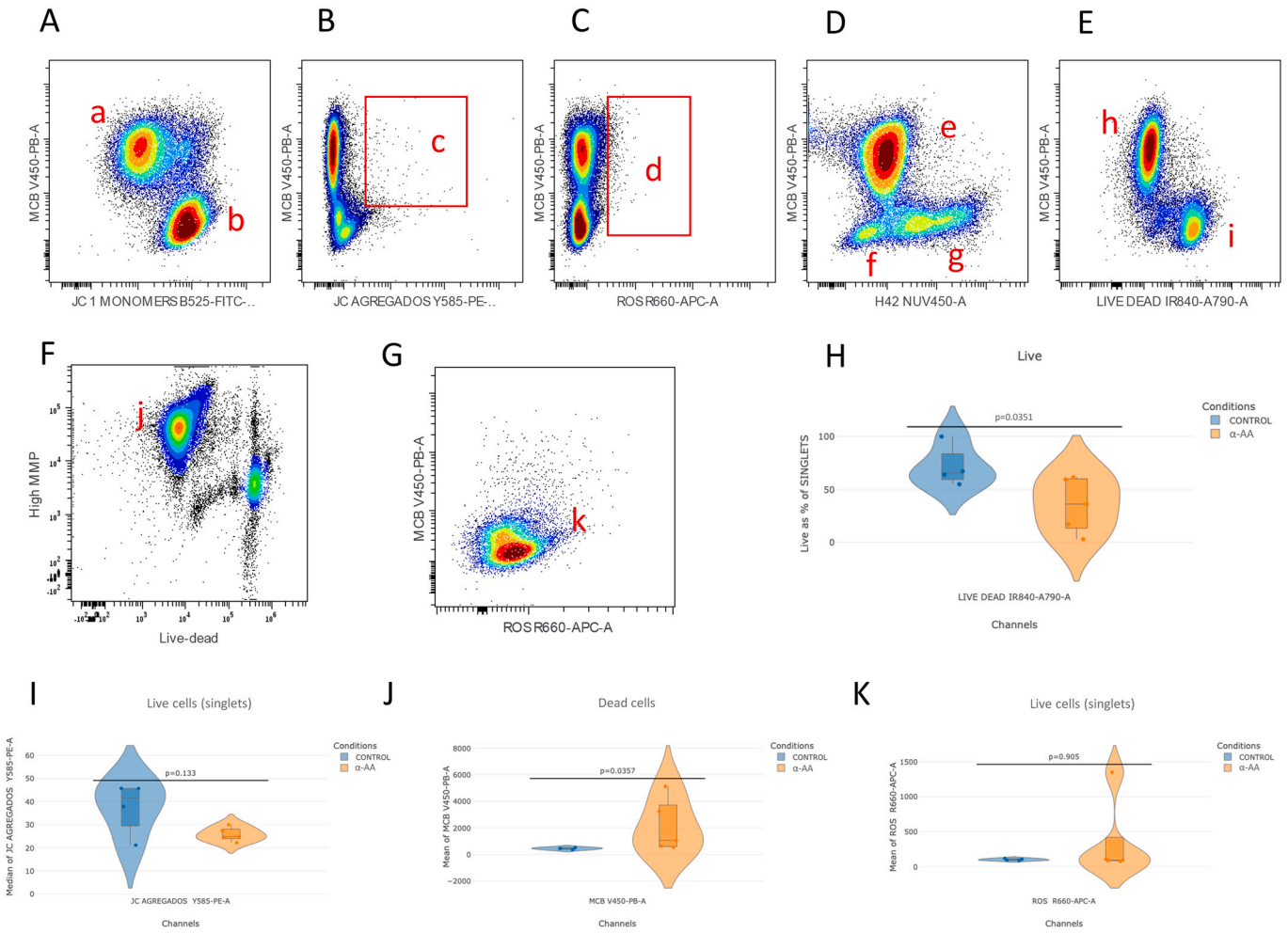

Fig. 1. Flow cytometry applied to the effect of α-AA exposure to differentiated human enterocytes. A) Cells showing significant amounts of GSH (a) and cells showing low mitochondrial activity (b); B) Dot plot showing in the Y-axis the MCB fluorescence corresponding to GSH, in the X-axis JC-1 aggregates fluorescence corresponding to highly active mitochondria (events in c); C) Dot plot showing in the Y-axis the MCB fluorescence corresponding to GSH, in the X-axis production of Reactive Oxygen Species (ROS) (events in d); D) Dot plot showing the GSH in cells (e) in relation to DNA positive events (f and g). Cells in g have increased membrane permeability; E) Dot plots showing live (h) and dead cells; F) Positive control for mitochondria showing high mitochondrial membrane potential (j) and positive controls for cells producing high amounts of ROS (k). H) Changes in viability; I) Changes in mitochondrial membrane potential in live cells; J) ROS in live cells; K) GSH content in dead cells.

The results from the molecular functions were consistent as the phosphorylative mechanism of sodium transmembrane transporter activity and the phosphorylate mechanism of potassium transmembrane transporter activity, reduced in quantity in protein ATP1A1 again (Fig. 2B and Supplementary Table S3). Together with protein kinase C alpha type (PRKCA), which appears only in control cells, protein ATP1A1 is implicated in cell communication by electrical coupling (Supplementary Table S2). The lower amount of ATP1A1 is also involved in glucocorticoid biosynthetic and metabolic processes, in steroid hormone binding and the cell responses to glycoside (Supplementary Tables S2 and S3). Phosphorylative mechanism of calcium transmembrane transporter activity was also affected by α-AA (Supplementary Table S3) In this case, the protein sarcoplasmic/endoplasmic reticulum calcium ATPase subunit alpha-2 (ATP2A2; Fold change: 0.73) (Table 1 and Supplementary Table S1), concerned with the ATPase sarcoplasmic/endoplasmic reticulum Ca^{2+} transporting, were found to be in lower abundance in α-AA treated cells. ADP binding (Supplementary Table S3) was found to be reduced in proteins such as ATP1A1, mitochondrial glutamate dehydrogenase 1 (GLUD1; Fold change: 0.79), mitochondrial glutamate dehydrogenase 2 (GLUD2; Fold change: 0.79), NADP-dependent malic enzyme, (ME1; Fold change: 0.62) and the regulatory gamma subunit of 5'-AMP-activated protein kinase (PRKAG1, which appears only in control) (Supplementary Table S1).

3.2.1.2. Nucleoside bisphosphate metabolic process. In this group, the exposure to α-AA led to a significant decrease of proteins involved in acetyl-CoA biosynthetic and metabolic processes in different pathways. Proteins acetyl-coenzyme A synthetase (ACSS2, only in control), lactate dehydrogenase (LDHD, Fold change: 0.73), liver carboxylesterase (CES1, Fold change: 0.67), mitochondrial malonyl-CoA decarboxylase (MLYCD, Fold change: 0.82), (Dihydrolipoyllysine-residue mitochondrial succinyltransferase component of 2-oxoglutarate dehydrogenase complex (DLST, Fold change: 0.81) and catalase (CAT, Fold change: 0.64) were found in lower quantity in cells exposed to α-AA (Table 1 and Supplementary Tables S1 and S2). Mitochondrial methylcrotonoyl-CoA carboxylase beta chain (MCCC2, Fold change: 0.72) and 3-hydroxyacyl-CoA dehydrogenase type-2 (HSD17B10, Fold change: 0.71), involved in branched-amino acid metabolic and catabolic processes (Table 1 and Supplementary Tables S1 and S2), were also diminished in α-AA treated cells.

3.2.1.3. Cellular amino acid metabolic process. Proteins involved in cellular amino acid metabolic process were found at lower concentrations in α-AA-treated cells compared to control cells ($p < 0.01$) (Fig. 2A).

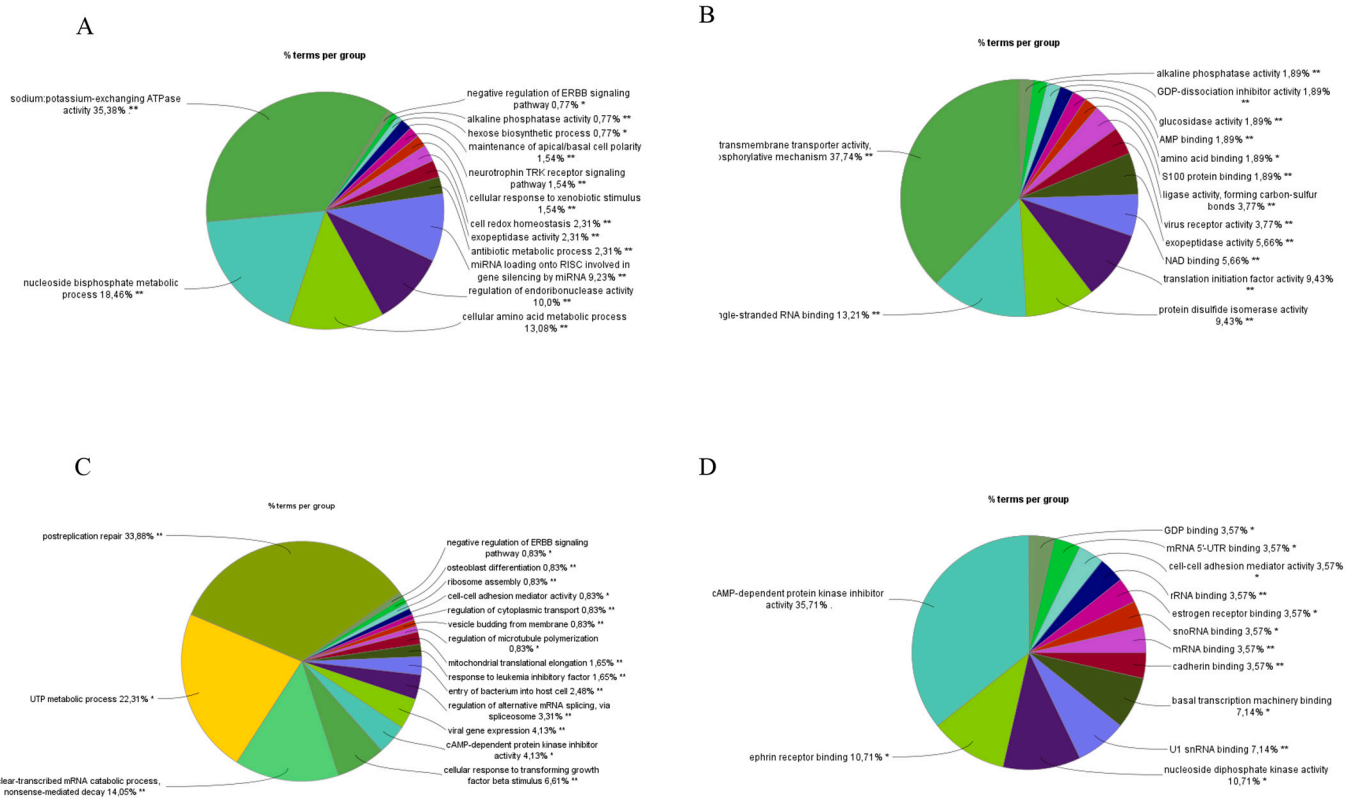

Fig. 2. Percentages of proteins annotated by Gene Ontology (* $p < 0.05$, ** $p < 0.01$) found in lower relative quantity in biological processes (A) and molecular functions (B), and percentages of proteins found in higher relative quantity in biological processes (C) and molecular functions (D) on differentiated human enterocytes as affected by exposure to 200 μM α-AA for 72 h.

Particularly, in the term tricarboxylic acid metabolic process, GLUD1 is lowered in abundance together with argininosuccinate synthase (ASS1, Fold change: 0.71), isocitrate dehydrogenase (IDH2, Fold change: 0.64) and iron-responsive element-binding protein 2 (IREB2, only in control) (Table 1 and Supplementary Tables S1 and S2). Glutamine family amino acid biosynthetic process is also found reduced, represented by proteins such as GLUD1, GLUD2 and ASS1 (Supplementary Table S1). On the other hand, certain proteins of the aspartate family amino acid metabolic process were found in lower quantity such as alkaline phosphatase placental type (ALPP, only in control), ASS1, DLST, procollagen-lysine, 2-oxoglutarate 5-dioxygenase 2 (PLOD2, only in control) and LDHD (Table 1 and Supplementary Tables S1 and S2). Within molecular functions, NAD-binding was found in lower quantity in proteins such as GLUD1 and IDH2 (Supplementary Table S3), where NAD is required as coenzyme. Furthermore, in amino acid binding, proteins GLUD1, GLUD2 and ASS1 were the only found in lower abundance in this process (Supplementary Table S3). On the other hand, proteins with oxidoreductase activity and NAD or NADP as proton acceptors, such as alcohol dehydrogenase 4 (ADH4, only in control), aldo-keto reductase family 1 member C2, (AKR1C2, Fold change: 0.50), aflatoxin B1 aldehyde reductase member 3 (AKR7A3, only in control) and dehydrogenase/reductase SDR family member 11 (DHRS11, Fold change: 0.69) (Table 1 and Supplementary Tables S1–S3), were found in decreased abundance in α-AA treated cells.

3.2.1.4. Protein disulfide isomerase activity. In both, biological processes and in molecular functions, proteins related with disulfide oxidoreductase activity (GSH activity) such as endoplasmic reticulum protein 44 (ERP44, Fold change: 0.81), protein disulfide isomerase A1 (P4HB, Fold change: 0.85), protein disulfide isomerase A3 (PDIA3, Fold change: 0.72), protein disulfide isomerase A4 (PDIA4, Fold change: 0.76) and glutathione S-transferase A2 (GSTA2, Fold change: 0.60) (Table 1 and Supplementary Tables S1–S3), were decreased in abundance in cells exposed to α-AA.

3.2.1.5. Regulation of endoribonuclease activity and miRNA loading onto RISC involved in gene silencing by miRNA. The exposure to α-AA caused a reduction in the abundance of chaperone related proteins such as the heat shock 70 kDa protein 1A (HSPA1A, Fold change: 0.76), heat shock 70 kDa protein 1B (HSPA1B, Fold change: 0.76), ATP-binding cassette, sub-family E, member 1, (ABCE1, Fold change: 0.57) and high mobility group protein B1, (HMGB1, Fold change: 0.74) (Table 1 and Supplementary Tables S1 and S2). Thus, within biological processes, proteins implicated in protein folding chaperone, protein folding in endoplasmic reticulum, endoribonuclease and ribonuclease activities were identified as the affected in proteins calreticulin (CALR, Fold change: 0.79), 78 kDa glucose-regulated protein (HSPA5, Fold change: 0.79) (Table 1 and Supplementary Table S1) and PDIA3 in addition to HSPA1A and HSPA1B (Supplementary Table S1).

Regarding miRNA (microRNA) loading onto RISC (miRNA-induce silencing complex), a number of AGO (argonaute) proteins were reduced in the presence of α-AA, namely AGO1, AGO2, AGO3 and AGO4 (all present only in control) (Table 1 and Supplementary Tables S1–S3).

3.2.1.6. Other proteins of biological significance found in lower relative quantity in α-AA-treated cells. Other significantly changed proteins found in lower quantity that have not been included in previous sections are tubulin beta-8 chain (TUBB8, Fold change: 0.15), intestinal sucrase-isomaltase, (SI, Fold change: 0.41), KDEL motif-containing protein 2 (KDELC2, Fold change: 0.47), 14–3-3 protein sigma (SFN, Fold change: 0.51) and glucosidase 2 subunit beta (PRKCSH, Fold change: 0.51) (Table 1 and Supplementary Table S1).

Proteins of biological significance only found in control samples are rootletin protein (CROCC), cilia- and flagella-associated protein 20

Table 1
Proteins from differentiated human enterocytes affected by the exposure to 200 μM α-AA for 72 h.

Protein name	Gene name	*p*-value	Fold-change[1]	Biological function	FASTA accession number
Protein kinase C alpha type	*PRKCA*	–	C	Cell communication by electrical coupling	J3KRN5
5'-AMP-activated protein kinase, regulatory gamma subunit	*PRKAG1*	–	C	ADP binding	F8VYY9
Acetyl-coenzyme A synthetase	*ACSS2*	–	C	Acetyl-CoA metabolic and biosynthetic processes	Q4G0E8
Alkaline phosphatase placental type	*ALPP*	–	C	Cellular amino acid metabolic process	B2R7C7
Iron-responsive element-binding protein 2	*IREB2*	–	C	Involved in tricarboxylic acid cycle	P48200
Procollagen-lysine,2-oxoglutarate 5-dioxygenase 2	*PLOD2*	–	C	Cellular amino acid metabolic process	E7ETU9
Alcohol dehydrogenase 4	*ADH4*	–	C	Oxidoreductase activity, acting on the CH-OH group of donors, NAD or NADP as acceptor	A0A024RDF8
Aflatoxin B1 aldehyde reductase member 3	*AKR7A3*	–	C	Oxidoreductase activity, acting on the CH-OH group of donors, NAD or NADP as acceptor	O95154
Protein argonaute-1, protein argonaute-2, protein argonaute-3, protein argonaute-4	*AGO1, AGO2, AGO3, AGO4*	–	C	miRNA loading onto RISC involved in gene silencing by miRNA	Q5TA58
Rootletin	*CROCC*	–	C	Internal structure of cilia and flagella	Q5TZA2
Cilia- and flagella-associated protein 20	*CFAP20*	–	C	Internal structure of cilia and flagella	Q9Y6A4
Ubiquitin carboxyl-terminal hydrolase isoenzyme L3	*UCHL3*	–	C	Deubiquitinating enzyme	P15374
Brain acid soluble protein 1	*BASP1*	–	C	Binding to protein kinase C alpha type	P80723
Endophilin-B2	*SH3GLB2*	–	C	Endosomal trafficking	Q9NR46
Cyclin-dependent kinase 2	*CDK2*	–	C	Entry in mitosis and DNA damage prevention	P24941
Caspase-3	*CASP3*	–	C	Apoptosis	P42574
Methionine aminopeptidase 1	*METAP1*	–	C	Normal progression through cell cycle	P53582
Cdc42-interacting protein 4	*STP*	–	C	Regulation of actin cytoskeleton	Q15642
Tubulin beta-8 chain	*TUBB8*	0.002	0.15	Structural constituent of cytoskeleton	Q3ZCM7
Sucrase-isomaltase, intestinal	*SI*	0.041	0.41	Hydrolyzing monosaccharides	P14410
KDEL motif-containing protein 2	*KDELC2*	0.039	0.47	Protein glycosidation	Q7Z4H8
Aldo-keto reductase family 1 member C2	*AKR1C2*	0.033	0.5	Oxidoreductase activity, acting on the CH-OH group of donors, NAD or NADP as acceptor	P52895
Glucosidase 2 subunit beta	*PRKCSH*	0.043	0.51	Glucosidase activity	K7ELL7
14–3-3 protein sigma	*SFN*	0.024	0.51	Cell cycle regulation and signal transduction	P31947
ATP-binding cassette sub-family E member 1	*ABCE1*	0.04	0.57	Regulation of *endo*- and ribonuclease activity	P61221
Glutathione S-transferase A2	*GSTA2*	0.0004	0.6	Protection against oxidative stress	P09210
NADP-dependent malic enzyme	*ME1*	0.0003	0.62	Oxidoreductase activity, acting on the CH-OH group of donors, NAD or NADP as acceptor	P48163
Isocitrate dehydrogenase	*IDH2*	0.002	0.64	Tricarboxylic acid metabolic process	P48735
Catalase	*CAT*	0.004	0.64	Cellular amino acid metabolic process/Protection against oxidative stress	P04040
Liver carboxylesterase	*CES1*	0.002	0.67	Acetyl-CoA metabolic and biosynthetic processes	P23141
Dehydrogenase/reductase SDR family member 11	*DHRS11*	0.001	0.69	Oxidoreductase activity, acting on the CH-OH group of donors, NAD or NADP as acceptor	Q6UWP2
3-hydroxyacyl-CoA dehydrogenase type-2	*HSD17B10*	0.026	0.71	Branched-amino acid metabolic and catabolic processes	Q99714
Argininosuccinate synthase	*ASS1*	0.019	0.71	Tricarboxylic acid metabolic process	Q5T6L4
Methylcrotonoyl-CoA carboxylase beta chain, mitochondrial	*MCCC2*	0.004	0.72	Branched-amino acid metabolic and catabolic processes	A0A140VK29
Sodium/potassium-transporting ATPase subunit alpha-1	*ATP1A1*	0.041	0.72	Establishment or maintenance of transmembrane electrochemical gradient	P05023
Protein disulfide isomerase A3	*PDIA3*	0.001	0.72	Protein disulfide isomerase activity	B3KQT9
Sarcoplasmic/endoplasmic reticulum calcium ATPase subunit alpha-2	*ATP2A2*	0.005	0.73	ATPase-coupled cation transmembrane transporter activity	A0A0S2Z3L2
Lactate dehydrogenase	*LDHD*	0.028	0.73	Acetyl-CoA metabolic and biosynthetic processes	Q86WU2
High mobility group protein B1	*HMGB1*	0.04	0.74	Interaction with nucleosomes, transcription factors, and histones	P09429
Protein disulfide isomerase A4	*PDIA4*	0.008	0.76	Protein disulfide isomerase activity	A0A090N8Y2
Heat shock 70 kDa protein 1A	*HSPA1A*	0.001	0.76	Regulation of endo- and ribonuclease activity; Protein folding chaperone	P0DMV8
Heat shock 70 kDa protein 1B	*HSPA1B*	0.001	0.76	Regulation of endo- and ribonuclease activity; Protein folding chaperone	A0A0G2JIW1
Glutamate dehydrogenase 1	*GLUD1*	0.002	0.79	Tricarboxylic acid cycle	P00367
Glutamate dehydrogenase 2	*GLUD2*	0.002	0.79	Tricarboxylic acid cycle	P49448
Calreticulin	*CALR*	0.002	0.79	Calcium-binding chaperone, protein folding chaperone in endoplasmic reticulum	P27797
78 kDa glucose-regulated protein	*HSPA5*	0.028	0.79	Protein folding in endoplasmic reticulum	P11021
Dihydrolipoyllysine-residue succinyltransferase	*DLST*	0.036	0.81	Tricarboxylic acid cycle	Q6IBS5
Endoplasmic reticulum protein 44	*ERP44*	0.035	0.81	Protein disulfide isomerase activity	Q9BS26
Malonyl-CoA decarboxylase, mitochondrial	*MLYCD*	0.037	0.82	Acetyl-CoA metabolic and biosynthetic processes	O95822
Protein disulfide isomerase A1	*P4HB*	0.019	0.85	Protein disulfide isomerase activity	B3KQT9
60S ribosomal protein L11	*RPL11*	0.027	1.25	Nuclear-transcribed mRNA catabolic process nonsense mediated decay	P62913
60S ribosomal protein L26	*RPL26*	0.004	1.33	Nuclear-transcribed mRNA catabolic process nonsense mediated decay	P61254
cAMP-dependent protein kinase type II-alpha regulatory subunit	*PRKAR2A*	0.045	1.35	cAMP-dependent protein kinase regulator activity	A0A0S2Z472

(*continued on next page*)

Table 1 (*continued*)

Protein name	Gene name	*p*-value	Fold-change[1]	Biological function	FASTA accession number
Microtubule-associated protein RP/EB family member 1	*MAPRE1*	0.005	1.4	Regulation of microtubule polymerization	Q15691
Ubiquitin carboxyl-terminal hydrolase 10	*USP10*	0.019	1.46	Postreplication repair	Q14694
Adenylate kinase 4	*AK4*	0.005	1.49	Synthesis of nucleotides and ribonucleotides triphosphate	P27144
60S ribosomal protein L12	*RPL12*	0.027	1.49	Nuclear-transcribed mRNA catabolic process nonsense mediated decay	P30050
Tubulin beta chain	*TUBB*	0.025	1.58	Structural constituent of cytoskeleton	P07437
Protein mago nashi homolog	*MAGOH*	0.009	1.6	Regulation of alternative mRNA splicing, via spliceosome	P61326
Proto-oncogene tyrosine-protein kinase Src	*SRC*	0.001	1.63	Regulation of actin cytoskeleton	P12931
Actin-related protein 2/3 complex subunit 4	*ARPC4*	0.043	1.67	Actin polymerization and DNA repair	P59998
U1 small nuclear ribonucleoprotein A	*SNRPA*	0.033	1.67	Regulation of alternative mRNA splicing, via spliceosome	P09012
Polyubiquitin B	*UBB*	0.002	1.68	Postreplication repair	B4DV12
Ubiquitin C	*UBC*	0.002	1.68	Postreplication repair	L8B196
Ubiquitin-60S ribosomal protein L40	*UBA52*	0.002	1.68	Postreplication repair	P62987
Ubiquitin- 40S ribosomal protein S27a	*RPS27A*	0.002	1.68	Postreplication repair	Q5RKT7
cAMP-dependent protein kinase type I-alpha regulatory subunit	*PRKAR1A*	0.022	1.71	cAMP-dependent protein kinase regulator activity	K7EPB2
Ras-related protein Rab-1B	*RAB1B*	0.026	1.75	Intracellular membrane trafficking	Q9H0U4
Replication factor C subunit 4	*RFC4*	0.018	1.77	Postreplication repair	P35249
RNA binding motif protein, X-linked-like-1	*RBMXL1*	0.02	1.78	Regulation of alternative mRNA splicing, via spliceosome	Q96E39
Serine/arginine-rich splicing factor 3	*SRSF3*	0.021	1.83	Regulation of alternative mRNA splicing, via spliceosome	P84103
40S ribosomal protein S25	*RPS25*	0.046	1.93	Nuclear-transcribed mRNA catabolic process nonsense mediated decay	P62851
Ubiquitin-conjugating enzyme E2 variant 1	*UBE2V1*	0.042	2.01	Postreplication repair	Q13404
Nucleoside-diphosphate kinase B	*NME2*	0.025	2.16	Synthesis of nucleotides and ribonucleotides triphosphate	P22392
Nucleoside-diphosphate kinase	*NME1-NME2*	0.025	2.16	Synthesis of nucleotides and ribonucleotides triphosphate	J3KPD9
Arfaptin-1	*ARFIP1*	0.009	2.35	Regulation of cytoplasmic transport	P53367
Serine/arginine-rich splicing factor 7	*SRSF7*	0.007	2.41	Regulation of alternative mRNA splicing, via spliceosome	Q16629
60S ribosomal protein L27a	*RPL27A*	0.006	2.72	Nuclear-transcribed mRNA catabolic process nonsense mediated decay	P46776
Profilin-1	*PFN1*	0.039	2.98	Regulation of cytoplasmic transport	P07737
40S ribosomal protein S10	*RPS10*	0.015	3.23	Nuclear-transcribed mRNA catabolic process nonsense mediated decay	P46783
40S ribosomal protein S18	*RPS18*	0.017	3.6	Nuclear-transcribed mRNA catabolic process nonsense mediated decay	P62269
28S ribosomal protein S27, mitochondrial	*MRPS27*	–	A	Mitochondrial translation and rRNA binding	Q8N6F2

[1] C: found only in control samples. A: found only in α-AA samples.

(CFAP20), ubiquitin carboxyl-terminal hydrolase isoenzyme L3 (UCHL3), brain acid soluble protein 1 (BASP1), endophilin-B2 (SH3GLB2), cyclin-dependent kinase 2 (CDK2), caspase-3 (CASP3), methionine aminopeptidase 1 (METAP1) and cdc42-interacting protein 4 (STP) (Table 1 and Supplementary Table S1).

3.2.2. *Proteins found in higher relative quantity in CACO-2 cells exposed to α-AA*

3.2.2.1. cAMP-dependent protein kinase inhibitor activity. Within molecular functions, the cAMP-dependent protein kinase (PKA) inhibitor activity was one of the most affected by the presence of α-AA (Fig. 2D). Namely, proteins such as alpha regulatory subunits of cAMP-dependent protein kinases type I (PRKAR1A, Fold change: 1.71), and type II (PRKAR2A, Fold change: 1.35) (Table 1 and Supplementary Tables S1–S5) were significantly increased in abundance in α-AA treated cells.

3.2.2.2. Post-replication repair. Within biological processes, proteins involved in post-replication repair increased in α-AA-treated cells as compared to control samples with this process being among the most affected in α-AA treated cells (Fig. 2C). Proteins such as the ubiquitin-conjugating enzyme E2 variant 1 (UBE2V1, Fold change: 2.01), the subunit 4 of replication factor C (RFC4, Fold change: 1.77), the ubiquitin-40S ribosomal protein S27a (RPS27A, Fold change: 1.68), the ubiquitin-60S ribosomal protein L40 (UBA52, Fold change: 1.68), the polyubiquitin B (UBB, Fold change: 1.68), the ubiquitin C (UBC, Fold change: 1.68), and the ubiquitin carboxyl-terminal hydrolase 10 (USP10, Fold change: 1,46) (Table 1 and Supplementary Tables S1–S4) were particularly affected. All these proteins are part of the ubiquitin system.

3.2.2.3. UTP metabolic process. Processes related to UTP metabolic process and the metabolism and synthesis of triphosphate nucleotides and ribonucleotides were also significantly affected by the exposure to α-AA (Fig. 2C and D). A number of proteins belonging to these processes were found in higher abundance in α-AA-treated cells compared to the control counterparts ($p < 0.05$), including nucleoside-diphosphate kinase (NME1-NME2, Fold change: 2.16) and nucleoside-diphosphate kinase B (NME2, Fold change: 2.16) and adenylate kinase 4 (AK4, Fold change: 1.49) (Table 1 and Supplementary Tables S1–S4).

3.2.2.4. Nuclear-transcribed mRNA catabolic process nonsense mediated decay. Proteins involved in nuclear-transcribed mRNA catabolic process nonsense mediated decay were in higher abundance in α-AA-treated cells compared to control samples ($p < 0.01$) (Fig. 2C). All the proteins

that appear in this process are implicated in 60s ribosomal proteins and 40s ribosomal proteins such as 40S ribosomal protein S18 (RPS18, Fold change: 3.60), 40S ribosomal protein S10 (RPS10, Fold change: 3.23), 60S ribosomal protein L27a (RPL27A, Fold change: 2.72), 40S ribosomal protein S25 (RPS25, Fold change: 1.93), 60S ribosomal protein L12 (RPL12, Fold change: 1.49), 60S ribosomal protein L26 (RPL26, Fold change: 1.33) and 60S ribosomal protein L11 (RPL11, Fold change: 1.25) (Table 1 and Supplementary Tables S1–S4) among others.

3.2.2.5. U1 snRNA binding and regulation of alternative mRNA splicing. In both, molecular functions and biological processes, proteins implicated in U1 snRNA (small nuclear RNA) binding, were found in higher quantity in α-AA treated cells. Proteins such as serine/arginine-rich splicing factor 7 (SRSF7, Fold change: 2.41), serine/arginine-rich splicing factor 3 (SRSF3, Fold change: 1.83), x-linked-like-1 RNA binding motif protein, (RBMXL1, Fold change: 1.78), U1 small nuclear ribonucleoprotein A (SNRPA, Fold change: 1.67) and protein mago nashi homolog (MAGOH, Fold change: 1.60) are involved in U1 snRNA binding and regulation of alternative mRNA splicing, via spliceosome (Table 1 and Supplementary Tables S1–S5).

3.2.2.6. Other proteins of biological significance found in higher relative quantity in α-AA-treated cells. The concentrations of several proteins implicated in these processes, such as profilin-1 (PFN1, Fold change: 2.98), arfaptin-1 (ARFIP1, Fold change: 2.35), ras-related protein Rab-1B (RAB1B, Fold change: 1.75), subunit 4 of actin-related protein 2/3 complex (ARPC4, Fold change: 1.67), proto-oncogene tyrosine-protein kinase Src (SRC, Fold change: 1.63), tubulin beta chain (TUBB, Fold change: 1.58) and microtubule-associated protein RP/EB family member 1 (MAPRE1, Fold change: 1.40) (Table 1 and Supplementary Tables S1–S5), were significantly increased in α-AA treated cells as compared to the control counterparts. The mitochondrial 28S ribosomal protein S27 (MRPS27) (Table 1 and Supplementary Table S1) was only found in the proteome of enterocytes exposed to α-AA.

4. Discussion

Oxidative stress is a condition that has been studied for years and is associated with multiple health disorders. Dietary oxidized lipids and proteins are known to impair the redox status in humans and contribute to such pathological conditions [12]. Yet, the underlying molecular pathways implicated in the toxicological effects of individual oxidized amino acids are poorly understood. While the pathophysiological effects of lipid oxidation products such as malondialdehyde (MDA) and 4-hydroxy nonenal (4-HNE) have been studied at a molecular level [26] the mechanisms by which oxidized proteins and amino acids could impair cell homeostasis is wholly unknown. This is of scientific relevance since oxidized amino acids such as α-AA, are commonly found in processed and red meat products that are, in turn, involved in the occurrence of postprandial, oxidative stress in the gastrointestinal tract and chronic inflammation processes [27,28]. As follows, the most relevant biological impairments caused by α-AA in differentiated human enterocytes are discussed. Fig. 3 illustrates the biological processes and metabolic pathways affected in these cells by the exposure to α-AA.

4.1. Impact of α-AA on electrical homeostasis and transepithelial function

α-Catalytic subunits proteins of the different ATPases in the cell, such as α subunits of Na^+/K^+-ATPase and Ca^{2+}-ATPase were significantly reduced in abundance in the presence of α-AA. Therefore, the results

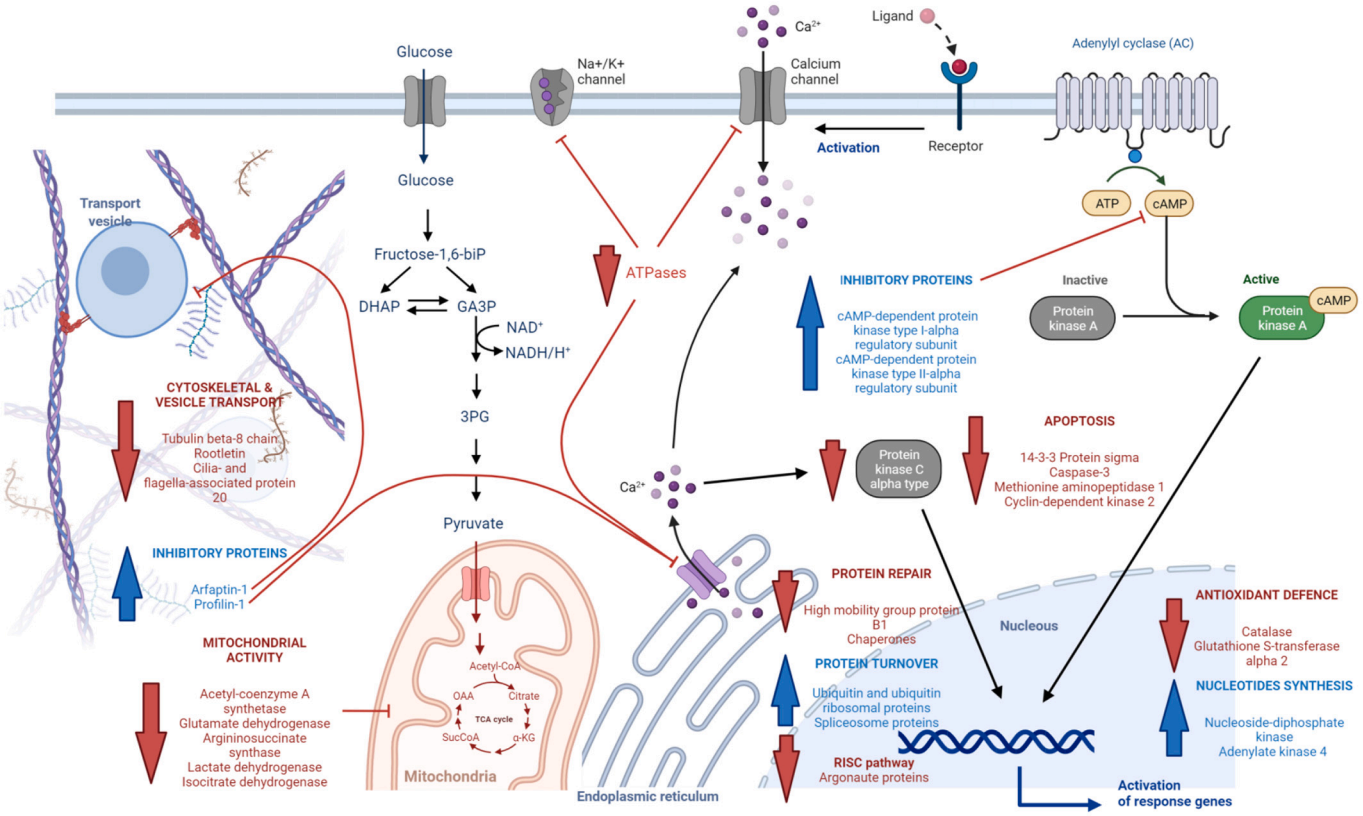

Fig. 3. Proposal of mechanisms underlying the cell toxicological effects of α-AA on differentiated human enterocytes. Upstream head blue arrows indicate higher concentration of proteins in α-AA treated cells. Downstream head red arrows indicate lower concentration of proteins in α-AA treated cells. Blunt head red arrows indicate an inhibited biological process or metabolic pathway. (For interpretation of the references to colour in this figure legend, the reader is referred to the web version of this article.)

suggest that these essential processes are partially suppressed in the presence of α-AA. The energy used in Na^+/K^+ exchange, maintains a physiological electrochemical gradient and disturbances in this fundamental cell function, may lead to health disorders [29]. The proteins involved in biological processes requiring glycosative reactions, were found to be in lower abundance or suppressed upon α-AA. For instance, glucocorticoid biosynthesis and related metabolic processes were diminished in the presence of α-AA, where glucocorticoids are steroid hormones synthesized in the intestinal mucosa by steroidogenic enzymes [30]. The response to glycosides was also impaired by the exposure to α-AA. Glycosides are secondary metabolites where a sugar moiety is linked to an aglycone molecule by an N-, S-, O- or C-glycosidic bond [31]. Glucose uptake, required for the synthesis of both glucocorticoids and glycosides, could have been affected by the disturbance of α-AA to the membrane Na^+/K^+ ATPase activity, as above mentioned. Therefore, an intracellular depletion of glucose caused by perturbation of Na^+/glucose cotransporters could explain an impairment of the biosynthesis of glucose-dependent molecules. The impairment of glucocorticoid metabolism could lead to physiological consequences as these hormones display anti-inflammatory local effects [32]. Thus, these results would be in line with other previous studies where α-AA was identified as a potential modulator of glucose homeostasis [6] and was associated with insulin resistance [7].

4.2. Cytoskeletal dynamics and vesicle transport

Tubulin is a structural constituent of cytoskeleton and forms microtubules in the cell, which have different functions such as maintenance of cell structure, protein trafficking and mitosis [33]. In this study, the occurrence of the protein tubulin beta-8 chain was significantly lower (Table 1 and Supplementary Table S1) in α-AA-treated cells, as compared to the control. Gilbert et al. [34] reported that the depolymerization of tubulin in enterocytes interfered in the displacement of apical proteins such as intestinal sucrase-isomaltase and the placental type alkaline phosphatase, which normally reaches a highly polarized apical distribution. A similar behavior was observed in sodium/potassium-transporting ATPase subunit alpha-1 in MCDK cells [35]. These results support the hypothesis that α-AA could act as an inhibitor of tubulin, which would in turn explain the lower concentration of intestinal sucrase-isomaltase and sodium/potassium-transporting ATPase subunit alpha-1, and the lack of placental type alkaline phosphatase, in cells treated with α-AA. Thus, α-AA affects the transport of these proteins within the cell, plausibly rendering them incapable of exerting their function in their cellular location.

Actin is another component of the cytoskeleton responsible for the transport of vesicles throughout the cytoplasm, among other functions [36]. The occurrence of proteins involved in the regulation of actin polymerization and vesicle transport, such as arfaptin-1, profilin-1, ras-related protein Rab-1B and proto-oncogene tyrosine-protein kinase Src, was significantly higher in α-AA-treated cells compared to the control. Huang et al. [37] reported that overexpression of arfaptin-1 inhibits vesicle transport while Shao et al. [38] found that profilin-1 inhibits actin polymerization. Furthermore, α-AA treated cells lacked several proteins such as endophilin-B2, which alters endosomal trafficking in vitro [39], Cdc42-interacting protein 4, involved in regulation of actin cytoskeleton [40] and the quantity of the protein glucosidase 2 subunit beta, an enzyme that cleaves glucose residues from nascent glycoproteins [41] was lowered. Thus, in this way, both actin polymerization and vesicle transport were inhibited processes, preventing the aforementioned proteins from correctly performing their function, as in the case of tubulin. Furthermore, profilin-1 inhibits the formation of IP3 (inositol trisphosphate) by binding to PIP2 (phosphatidylinositol 4,5-bisphosphate) [42], which is responsible for the release of calcium into the intracellular space activating protein kinase C alpha type. This is coherent with the present results as protein kinase C alpha type and brain acid soluble protein 1, were not found in α-AA treated cells. The results are also consistent with the lower abundance of sarcoplasmic/endoplasmic reticulum calcium ATPase subunit alpha-2 protein in α-AA treated cells compared to the control counterparts.

4.3. Impact of α-AA on energy metabolism and mitochondrial function

The disturbance of the energy metabolism caused by α-AA in intestinal cells may be caused by the impairment that such oxidized amino acid is able to induce at the mitochondrial level. Glutamate dehydrogenase (GDH) is a mitochondrial enzyme that catalyzes glutamate into 2-oxoglutarate (2-OG) [43], and it plays a major role in mitochondrial TCA cycle and energetic cell homeostasis. The exposure to α-AA significantly reduced the quantity of the two GDH isozymes. As mentioned in due course, other enzymes involved in acetyl-CoA biosynthesis and TCA cycle are also affected in cells exposed to α-AA, which corroborates the noxious effect of this oxidized amino acid in the energetic metabolism of the intestinal cell. Studies in pigs have shown that approximately 90% of dietary glutamate is metabolized in the intestine and 50% of it is oxidized to CO_2 [44]. This metabolic behavior not only fulfils intestinal cell energy demand, it is also necessary to keep the Na^+/K^+ ATPase pump active [45]. TCA cycle and Na^+/K^+ ATPases are interconnected processes because the energy obtained in TCA cycle is fundamental to keep the Na^+/K^+ ATPase pump active, and a direct and immediate consequence of Na+/K+ ATPase inhibition is the disruption of central carbon metabolism [46]. The mitochondrial disturbance of α-AA was already suggested by flow cytometry results, where a decrease in mitochondrial activity was revealed in cells exposed to α-AA, though not to a significant extent (Fig. 1I). The lower abundance of proteins such as glutamate dehydrogenase, NADP-dependent malic enzyme, 5'-AMP-activated protein kinase regulatory gamma subunit, isocitrate dehydrogenase and argininosuccinate synthase, is consistent with a decreased mitochondrial activity.

As anticipated, different proteins related to acetyl-CoA biosynthesis and TCA cycle such as glutamate dehydrogenase, isocitrate dehydrogenase and argininosuccinate synthase [47] were found in lower abundance in the presence of α-AA. This fact could have contributed to the significant decrease in mitochondrial activity through the impairment of the TCA cycle and other related pathways. Glutamine family amino acid biosynthetic process and aspartate family amino acid metabolic process were found to comprise proteins with lowered abundance such as glutamate dehydrogenase, argininosuccinate synthase and alkaline phosphatase placental type, argininosuccinate synthase, dihydrolipoyllysine-residue mitochondrial succinyltransferase, procollagen-lysine,2-oxoglutarate 5-dioxygenase 2 and lactate dehydrogenase, respectively. Proteins dihydrolipoyllysine-residue mitochondrial succinyltransferase and procollagen-lysine,2-oxoglutarate 5-dioxygenase 2, are particularly implicated in lysine degradation. Thus, as these proteins are found in lower abundance in the presence of α-AA, they can affect lysine degradation process and may be involved in accumulation of lysine in cell, which may lead to physiological impairments [48]. With α-AA being an oxidation product of lysine, the suppression of molecular mechanisms involved in lysine degradation seems reasonable.

4.4. Oxidative stress and antioxidant defenses

A decreased and inefficient mitochondrial activity is typically linked to ROS generation and the onset of oxidative stress [49]. In fact, da Silva et al. [10] reported a significant increase in ROS in rat neuronal cells as induced by α-AA. Consistently, in a previous study, the exposure of differentiated enterocytes to α-AA for 72 h led to ROS generation with respect to the control cells [11]. In our present study, such condition was not confirmed by the flow cytometry analysis. Yet, other analyses indicate the depletion of antioxidant defenses and the accretion of protein carbonyls in α-AA treated cells, with both conditions typically occurring under oxidative stress. The concentration of catalase, known to

counteract peroxides [50], was significantly lower in α-AA treated cells compared to the control counterparts. Other relevant oxidoreductases that could be involved in detoxifying dietary oxidation products such as alcohol dehydrogenase 4 and aflatoxin B1 aldehyde reductase member 3 [51] were not found in α-AA treated cells. These results indicate that certain antioxidant defenses were whether depleted in cells exposed to α-AA or that the antioxidant response in these cells failed to be appropriately activated.

On the other hand, glutathione (GSH) is a tetrapeptide with remarkable antioxidant activity in cells. While no apparent effect of α-AA was found in relation to GSH content in live cells (data not shown), da Silva et al. [10] found a significant depletion of GSH in the cerebral cortex of rats exposed to 4 mM of α-AA. In our previous study [11], the long-term exposure (72 h) of differentiated CACO-2 cells to 200 μM of α-AA had no effect on the occurrence of GSH. Interestingly in the population of dead cells, a significant increase in GSH concentration was observed, probably due to a compensatory increase in GSH after an oxidative insult (Fig. 1K), compared with control cells. Yet, this event is a reflection of a failed antioxidant response as the concentration of glutathione S-transferase alpha 2 (encoded by *GSTA2* gene) was lower in cells exposed to α-AA compared to the control cells. This enzyme detoxifies pro-oxidative substances by catalyzing the nucleophilic attack by GSH on electrophilic atoms of such reactive substrates [52]. Therefore, the synthesis and accretion of GSH in α-AA-exposed cells seemed inoperable without the timely involvement of the appropriate enzymes, with these cells eventually dying, still holding high concentrations of GSH. Additionally, Falkner et al. [53] reported that glucocorticoids regulate *GSTA2* gene in cultured rat hepatocytes, repressing its expression at low concentrations (10 to 100 nM) but promoting its expression at high concentrations (>1 μM). Hence, it is reasonable that the lower concentration of glutathione S-transferase A2 observed in this study, would reflect the lower quantity of proteins involved in glucocorticoid biosynthetic and metabolic processes.

4.5. Impact of α-AA on protein conformation, functionality and repair

Chaperone proteins are implicated in preventing aberrant protein folding and aggregations [54]. Proteins such as ATP-binding cassette sub-family E member 1, implicated in ribosome biogenesis, and chaperone proteins heat shock 70 kDa protein 1A and heat shock 70 kDa protein 1B [54], were found in lower quantity in cells exposed to α-AA. Moreover, the concentration of high mobility group protein B1 HMGB1, one of the most important chromatin proteins that interacts with nucleosomes, transcription factors and histones [55], was significantly lower in α-AA-treated cells compared to the control. Thus, α-AA may be contributing to the occurrence of aberrant protein conformations and impaired functionalities as denoted by the higher extent of protein carbonylation in α-AA-treated cells than in the control counterparts. The ubiquitin system plays a central role in protein homeostasis by regulating the turnover of proteins involved in processes such as signal transduction, DNA repair and apoptosis, among others [56]. In this study, the higher abundance of the ubiquitin-dependent degradation of proteins may respond to the disability of the chaperone system to repair aberrant proteins, which leads to increased occurrence of anomalous protein conformations. This result is consistent with the accretion of protein carbonyls and the lack of ubiquitin carboxyl-terminal hydrolase isozyme L3, a deubiquitinating enzyme [57].

Consistently, the nuclear-transcribed mRNA catabolic process nonsense mediated decay is found in higher quantity in α-AA-treated cells. The nonsense mediated decay pathway for nuclear-transcribed mRNAs prevents the translation of such mRNA into truncated and potentially harmful proteins [58]. The higher abundance of proteins involved in this pathway could prevents the formation of truncated and potentially harmful proteins while U1 snRNA binding protein (part of the spliceosome) is as well found increased in quantity, probably to remove misfolded or truncated proteins. The results from a previous study [11] are consistent with the present ones in regards to α-AA promoting the oxidative damage to cell proteins. The present results show an attempt of the cell to revert these modifications in proteins. Thus, all the processes in which proteins are in higher abundance are aimed to DNA repair, and others are associated with mechanisms to prevent truncated proteins. This is also linked to the lower abundance of proteins argonaute (AGO), that are responsible for repressing miRNA translation [59]. The lower abundance of these proteins in α-AA-treated cells in conjunction with the higher quantity of proteins involved in nucleoside and ribonucleoside biosynthetic and metabolic processes, support the hypothesis that the RISC complex is repressed. This would enable the expression of non-silencing genes and therefore, facilitate the synthesis of new non-truncated proteins.

4.6. Impact of α-AA on stress response, apoptosis and cell cycle

Intestinal cells display a number of biochemical mechanisms to maintain homeostasis and response against physical, biological and chemical threats. PKA plays an important role in the maintenance of cellular homeostatic processes, in cell metabolism and in the intracellular signal transduction process [60]. In this study, the regulatory subunits of PKA, which regulate the cAMP-PKA binding process, are upwardly inhibited in cells exposed to α-AA. Therefore, the effect of α-AA on inhibiting the multiple functions in which PKA is involved, may lead to various impaired physiological processes including a suitable cell response against this chemical threat. This may affect, among others, to the ability of the cell to shift their gene expression patterns and activate, as a result, defense mechanisms under stress conditions [61]. On this line, miRNA is assembled with AGO proteins to form the RNA-induced silencing complex (RISC), which pairs with target miRNAs and represses their expression [59]. α-AA significantly affected this regulation process by downregulating genes encoding argonaute proteins (AGO1, AGO2, AGO3 and AGO4).

Regarding cell cycle regulation and apoptosis, certain proteins involved in these processes were at significantly lower concentrations, or were not found, in α-AA treated cells. Among these, we may cite 14–3-3 protein sigma, caspase-3, methionine aminopeptidase 1 and cyclin-dependent kinase 2. These results, as well as those from flow cytometer, indicate that α-AA affects cell viability. Yet, this condition does not seem to be manifested in a high quantity of proteins implicated in apoptosis, but rather to a lower abundance of those involved in a suitable maintenance of cell cycle.

Finally, as aforementioned, one protein, 28S ribosomal protein S27 mitochondrial, was found only in α-AA-treated cells. This protein is a RNA-binding component that is involved in mitochondrial protein synthesis and in biogenesis and maintenance of organelles [62]. This is consistent with the hypothesis of the stimulation of protein synthesis α-AA-treated cells in order to maintain homeostasis and prevent apoptosis.

5. Conclusion

This paper described, for the first time, the underlying mechanisms of the biological impairments caused by the oxidized amino acid, α-AA, on differentiated human enterocytes. The analysis of the proteome suggests that lysine oxidation end-product alters cell homeostasis through a variety of mechanisms that include transepithelial transportation, energy supply and vesicle transportation of proteins. While certain antioxidant defenses and repair mechanisms are diminished by the α-AA, the cell activates protein turn-over mechanisms to avoid apoptosis. These results emphasize the role of dietary oxidized amino acids in intestinal cell physiology and provides grounds to unveil, in further studies, the impact of this and other protein oxidation products in intestinal pathological conditions.

Declaration of Competing Interest

The authors declare that they have no known competing financial interests or personal relationships that could have appeared to influence the work reported in this paper.

Acknowledgements

The financial support from the Spanish Ministry of Economics and Competitiveness (SMEC) is acknowledged (project number AGL2017-84586-R). The "Junta de Extremadura/FEDER" is also acknowledged for financial support (grant number GR108104). S. Díaz-Velasco is recipient of a fellowship from the Spanish Ministry of Science, Innovation and Universities (PRE2018-084001).

Appendix A. Supplementary data

Supplementary data to this article can be found online at https://doi.org/10.1016/j.bbapap.2022.140797.

References

[1] B.S. Berlett, E.R. Stadtman, Protein oxidation in aging, disease, and oxidative stress, J. Biol. Chem. 272 (1997) 20313–20316, https://doi.org/10.1074/jbc.272.33.20313.
[2] J.M. Dos Santos, S. Tewari, R.H. Mendes, The role of oxidative stress in the development of diabetes mellitus and its complications, J. Diabetes Res. 2019 (2019), https://doi.org/10.1155/2019/4189813.
[3] A.R. Bourgonje, M. Feelisch, K.N. Faber, A. Pasch, G. Dijkstra, H. van Goor, Oxidative stress and redox-modulating therapeutics in inflammatory bowel disease, Trends Mol. Med. 26 (2020) 1034–1046, https://doi.org/10.1016/j.molmed.2020.06.006.
[4] W.Q. Chen, W.S. Lian, Y.F. Yuan, M.Q. Li, The synergistic effects of oxaliplatin and piperlongumine on colorectal cancer are mediated by oxidative stress, Cell Death Dis. 10 (2019) 1–12, https://doi.org/10.1038/s41419-019-1824-6.
[5] D.R. Sell, C.M. Strauch, W. Shen, V.M. Monnier, 2-Aminoadipic acid is a marker of protein carbonyl oxidation in the aging human skin: effects of diabetes, renal failure and sepsis, Biochem. J. 404 (2007) 269–277, https://doi.org/10.1042/BJ20061645.
[6] T.J. Wang, D. Ngo, N. Psychogios, A. Dejam, M.G. Larson, R.S. Vasan, A. Ghorbani, J. O'Sullivan, S. Cheng, E.P. Rhee, S. Sinha, E. McCabe, C.S. Fox, C.J. O'Donnell, J. E. Ho, J.C. Florez, M. Magnusson, K.A. Pierce, A.L. Souza, Y. Yu, C. Carter, P. E. Light, O. Melander, C.B. Clish, R.E. Gerszten, 2-Aminoadipic acid is a biomarker for diabetes risk, J. Clin. Invest. 123 (2013) 4309–4317, https://doi.org/10.1172/JCI64801.
[7] H.J. Lee, H.B. Jang, W.H. Kim, K.J. Park, K.Y. Kim, S.I. Park, H.J. Lee, 2-Aminoadipic acid (2-AAA) as a potential biomarker for insulin resistance in childhood obesity, Sci. Rep. 9 (2019) 1–10, https://doi.org/10.1038/s41598-019-49578-z.
[8] M. Estaras, F.Z. Ameur, M. Estévez, S. Díaz-Velasco, A. Gonzalez, The lysine derivative aminoadipic acid, a biomarker of protein oxidation and diabetes-risk, induces production of reactive oxygen species and impairs trypsin secretion in mouse pancreatic acinar cells, Food Chem. Toxicol. 145 (2020), 111594, https://doi.org/10.1016/j.fct.2020.111594.
[9] D.R. Brown, H.A. Kretzschmar, The glio-toxic mechanism of α-aminoadipic acid on cultured astrocytes, J. Neurocytol. 27 (1998) 109–118, https://doi.org/10.1023/A:1006947322342.
[10] J.C. da Silva, A.U. Amaral, C. Cecatto, A. Wajner, K. dos Santos Godoy, R. T. Ribeiro, A. de Mello Gonçalves, Â. Zanatta, M.S. da Rosa, S.O. Loureiro, C. R. Vargas, G. Leipnitz, D.O.G. de Souza, M. Wajner, α-Ketoadipic acid and α-aminoadipic acid cause disturbance of glutamatergic neurotransmission and induction of oxidative stress in vitro in brain of adolescent rats, Neurotox. Res. 32 (2017) 276–290, https://doi.org/10.1007/s12640-017-9735-8.
[11] S. Díaz-Velasco, A. González, F.J. Peña, M. Estévez, Noxious effects of selected food-occurring oxidized amino acids on differentiated CACO-2 intestinal human cells, Food Chem. Toxicol. 144 (2020) 1–8, https://doi.org/10.1016/j.fct.2020.111650.
[12] M. Estévez, Y. Xiong, Intake of oxidized proteins and amino acids and causative oxidative stress and disease: recent scientific evidences and hypotheses, J. Food Sci. 84 (2019) 387–396, https://doi.org/10.1111/1750-3841.14460.
[13] M. Utrera, V. Parra, M. Estévez, Protein oxidation during frozen storage and subsequent processing of different beef muscles, Meat Sci. 96 (2014) 812–820, https://doi.org/10.1016/j.meatsci.2013.09.006.
[14] IARC, Carcinogenicity of consumption of red and processed meat, Lancet Oncol. 16 (2015) 1599–1600, https://doi.org/10.1016/S1470-2045(15)00444-1.
[15] M. Pinto, S. Robine Leon, M.D. Appay, Enterocyte-like differentiation and polarization of the human colon carcinoma cell line Caco-2 in culture, Biol. Cell. 47 (1983) 323–330.
[16] M. Utrera, M. Estévez, Oxidation of myofibrillar proteins and impaired functionality: underlying mechanisms of the carbonylation pathway, J. Agric. Food Chem. 60 (2012) 8002–8011, https://doi.org/10.1021/jf302111j.
[17] M. Timm-Heinrich, S. Eymard, C.P. Baron, H.H. Nielsen, C. Jacobsen, Oxidative changes during ice storage of rainbow trout (*Oncorhynchus mykiss*) fed different ratios of marine and vegetable feed ingredients, Food Chem. 136 (2013) 1220–1230, https://doi.org/10.1016/j.foodchem.2012.09.019.
[18] M. Utrera, M. Estévez, Oxidative damage to poultry, pork, and beef during frozen storage through the analysis of novel protein oxidation markers, J. Agric. Food Chem. 61 (2013) 7987–7993, https://doi.org/10.1021/jf402220q.
[19] J.M. Ortiz-Rodríguez, F.E. Martín-Cano, G.L. Gaitskell-Phillips, A. Silva, C. Ortega-Ferrusola, M.C. Gil, F.J. Peña, Low glucose and high pyruvate reduce the production of 2-oxoaldehydes, improving mitochondrial efficiency, redox regulation, and stallion sperm function†, Biol. Reprod. 105 (2021) 519–532, https://doi.org/10.1093/BIOLRE/IOAB073.
[20] P.M. Muñoz, C.O. Ferrusola, G. Vizuete, M.P. Dávila, H.R. Martinez, F.J. Peña, Depletion of intracellular thiols and increased production of 4-hydroxynonenal that occur during cryopreservation of stallion spermatozoa Lead to caspase activation, loss of motility, and cell death, Biol. Reprod. 93 (2015), https://doi.org/10.1095/BIOLREPROD.115.132878.
[21] M. Utrera, D. Morcuende, J.G. Rodríguez-Carpena, M. Estévez, Fluorescent HPLC for the detection of specific protein oxidation carbonyls - α-aminoadipic and γ-glutamic semialdehydes – in meat systems, Meat Sci. 89 (2011) 500–506, https://doi.org/10.1016/j.meatsci.2011.05.017.
[22] M. Akagawa, T. Sasaki, K. Suyama, Oxidative deamination of lysine residue in plasma protein of diabetic rats: novel mechanism via the Maillard reaction, Eur. J. Biochem. 269 (2002) 5451–5458, https://doi.org/10.1046/j.1432-1033.2002.03243.x.
[23] A. Shevchenko, H. Tomas, J. Havliš, J.V. Olsen, M. Mann, In-gel digestion for mass spectrometric characterization of proteins and proteomes, Nat. Protoc. 1 (2007) 2856–2860, https://doi.org/10.1038/nprot.2006.468.
[24] J. Delgado, F. Núñez, M.A. Asensio, R.A. Owens, Quantitative proteomic profiling of ochratoxin a repression in Penicillium nordicum by protective cultures, Int. J. Food Microbiol. 305 (2019), 108243, https://doi.org/10.1016/j.ijfoodmicro.2019.108243.
[25] G. Bindea, B. Mlecnik, H. Hackl, P. Charoentong, M. Tosolini, A. Kirilovsky, W.-H. Fridman, F. Pagès, Z. Trajanoski, J. Galon, ClueGO: a Cytoscape plug-in to decipher functionally grouped gene ontology and pathway annotation networks, Bioinformatics. 25 (2009) 1091–1093, https://doi.org/10.1093/bioinformatics/btp101.
[26] A. Ayala, M.F. Muñoz, S. Argüelles, Lipid peroxidation: production, metabolism, and signaling mechanisms of malondialdehyde and 4-hydroxy-2-nonenal, Oxidative Med. Cell. Longev. 2014 (2014), https://doi.org/10.1155/2014/360438.
[27] J. Kanner, J. Selhub, A. Shpaizer, B. Rabkin, I. Shacham, O. Tirosh, Redox homeostasis in stomach medium by foods: the postprandial oxidative stress index (POSI) for balancing nutrition and human health, Redox Biol. 12 (2017) 929–936, https://doi.org/10.1016/j.redox.2017.04.029.
[28] D. de La Pomélie, V. Santé-Lhoutellier, T. Sayd, P. Gatellier, Oxidation and nitrosation of meat proteins under gastro-intestinal conditions: consequences in terms of nutritional and health values of meat, Food Chem. 243 (2018) 295–304, https://doi.org/10.1016/j.foodchem.2017.09.135.
[29] A.N. Shrivastava, A. Triller, R. Melki, Cell biology and dynamics of neuronal Na+/K+-ATPase in health and diseases, Neuropharmacology. 169 (2020), 107461, https://doi.org/10.1016/j.neuropharm.2018.12.008.
[30] I. Cima, N. Corazza, B. Dick, A. Fuhrer, S. Herren, S. Jakob, E. Ayuni, C. Mueller, T. Brunner, Intestinal epithelial cells synthesize glucocorticoids and regulate T cell activation, J. Exp. Med. 200 (2004) 1635–1646, https://doi.org/10.1084/jem.20031958.
[31] K.B. Louie, S.M. Kosina, Y. Hu, H. Otani, M. de Raad, A.N. Kuftin, N.J. Mouncey, B. P. Bowen, T.R. Northen, Mass spectrometry for natural product discovery, in: Compr. Nat. Prod. III, Elsevier, 2020, pp. 263–306, https://doi.org/10.1016/b978-0-12-409547-2.14834-6.
[32] A.E. Coutinho, K.E. Chapman, The anti-inflammatory and immunosuppressive effects of glucocorticoids, recent developments and mechanistic insights, Mol. Cell. Endocrinol. 335 (2011) 2–13, https://doi.org/10.1016/j.mce.2010.04.005.
[33] R.A. Stanton, K.M. Gernert, J.H. Nettles, R. Aneja, Drugs that target dynamic microtubules: a new molecular perspective, Med. Res. Rev. 31 (2011) 443–481, https://doi.org/10.1002/med.20242.
[34] T. Gilbert, A. Le Bivic, A. Quaroni, E. Rodriguez-Boulan, Microtubular organization and its involvement in the biogenetic pathways of plasma membrane proteins in Caco-2 intestinal epithelial cells, J. Cell Biol. 113 (1991) 275–288, https://doi.org/10.1083/jcb.113.2.275.
[35] M.J. Caplan, H.C. Anderson, G.E. Palade, J.D. Jamieson, Intracellular sorting and polarized cell surface delivery of (Na+,K+)ATPase, an endogenous component of MDCK cell basolateral plasma membranes, Cell. 46 (1986) 623–631, https://doi.org/10.1016/0092-8674(86)90888-3.
[36] S.R. Goodman, W.E. Zimmer, Cytoskeleton, in: Med. Cell Biol., Third ed., Elsevier Inc., 2007, pp. 59–100, https://doi.org/10.1016/B978-0-12-370458-0.50008-6.
[37] L.H. Huang, W.C. Lee, S.T. You, C.C. Cheng, C.J. Yu, Arfaptin-1 negatively regulates Arl1- mediated retrograde transport, PLoS One 10 (2015), https://doi.org/10.1371/journal.pone.0118743.
[38] J. Shao, W.J. Welch, N.A. DiProspero, M.I. Diamond, Phosphorylation of profilin by ROCK1 regulates polyglutamine aggregation, Mol. Cell. Biol. 28 (2008) 5196–5208, https://doi.org/10.1128/mcb.00079-08.

[39] J.M. Serfass, Y. Takahashi, Z. Zhou, Y.I. Kawasawa, Y. Liu, N. Tsotakos, M. M. Young, Z. Tang, L. Yang, J.M. Atkinson, Z.C. Chroneos, H.G. Wang, Endophilin B2 facilitates endosome maturation in response to growth factor stimulation, autophagy induction, and influenza A virus infection, J. Biol. Chem. 292 (2017) 10097–10111, https://doi.org/10.1074/jbc.M117.792747.
[40] T. Itoh, K.S. Erdmann, A. Roux, B. Habermann, H. Werner, P. De Camilli, Dynamin and the actin cytoskeleton cooperatively regulate plasma membrane invagination by BAR and F-BAR proteins, Dev. Cell 9 (2005) 791–804, https://doi.org/10.1016/J.DEVCEL.2005.11.005.
[41] M.F. Pelletier, A. Marcil, G. Sevigny, C.A. Jakob, D.C. Tessier, E. Chevet, R. Menard, J.J.M. Bergeron, D.Y. Thomas, The heterodimeric structure of glucosidase II is required for its activity, solubility, and localization in vivo, Glycobiology. 10 (2000) 815–827, https://doi.org/10.1093/glycob/10.8.815.
[42] P.J. Goldschmidt-Clermont, L.M. Machesky, J.J. Baldassare, T.D. Pollard, The actin-binding protein profilin binds to PIP2 and inhibits its hydrolysis by phospholipase C, Science (80-.) 247 (1990) 1575–1578, https://doi.org/10.1126/science.2157283.
[43] M. Monné, A. Vozza, F.M. Lasorsa, V. Porcelli, F. Palmieri, Mitochondrial carriers for aspartate, glutamate and other amino acids: a review, Int. J. Mol. Sci. 20 (2019) 4456, https://doi.org/10.3390/ijms20184456.
[44] B. Stoll, D.G. Burrin, J. Henry, H. Yu, F. Jahoor, P.J. Reeds, Substrate oxidation by the portal drained viscera of fed piglets, Am. J. Physiol. Endocrinol. Metab. 277 (1999), https://doi.org/10.1152/ajpendo.1999.277.1.e168.
[45] P. Vaugelade, L. Posho, B. Darcy-Vrillon, F. Bernard, M.T. Morel, P.H. Duée, Intestinal oxygen uptake and glucose metabolism during nutrient absorption in the pig, Proc. Soc. Exp. Biol. Med. 207 (1994) 309–316, https://doi.org/10.3181/00379727-207-43821.
[46] S.M. Sanderson, Z. Xiao, A.J. Wisdom, S. Bose, M.V. Liberti, M.A. Reid, E. Hocke, S. G. Gregory, D.G. Kirsch, J.W. Locasale, The Na+/K+ ATPase regulates glycolysis and modifies immune metabolism in tumors, BioRxiv. (2020), https://doi.org/10.1101/2020.03.31.018739.
[47] P. Prasun, Disorders of pyruvate metabolism and tricarboxylic acid cycle, in: Mitochondrial Med., Elsevier, 2019, pp. 83–95, https://doi.org/10.1016/b978-0-12-817006-9.00015-0.
[48] J. Bouchereau, M. Schiff, Inherited disorders of lysine metabolism: a review, J. Nutr. 150 (2020) 2556S–2560S, https://doi.org/10.1093/jn/nxaa112.
[49] S. Kausar, F. Wang, H. Cui, The role of mitochondria in reactive oxygen species generation and its implications for neurodegenerative diseases, Cells. 7 (2018) 274, https://doi.org/10.3390/cells7120274.
[50] M. Schieber, N.S. Chandel, ROS function in redox signaling and oxidative stress, Curr. Biol. 24 (2014) R453–R462, https://doi.org/10.1016/j.cub.2014.03.034.
[51] K.M. Schaich, Toxicity of lipid oxidation products consumed in the diet, Bailey's Ind. Oil Fat. Prod. (2020) 1–88, https://doi.org/10.1002/047167849X.BIO116.
[52] K.W. Kang, S.H. Choi, S.G. Kim, Peroxynitrite activates nf-e2-related factor 2/antioxidant response element through the pathway of phosphatidylinositol 3-kinase: the role of nitric oxide synthase in rat glutathione S-transferase A2 induction, Nitric Oxide Biol. Chem. 7 (2002) 244–253, https://doi.org/10.1016/S1089-8603(02)00117-9.
[53] K.C. Falkner, J.A. Pinaire, G.-H. Xiao, T.E. Geoghegan, R.A. Prough, Regulation of the rat glutathione S-transferase A2 gene by glucocorticoids: involvement of both the glucocorticoid and Pregnane X receptors, Mol. Pharmacol. 60 (2001).
[54] H. Saibil, Chaperone machines for protein folding, unfolding and disaggregation, Nat. Rev. Mol. Cell Biol. 14 (2013) 630–642, https://doi.org/10.1038/nrm3658.
[55] M.E. Bianchi, A. Agresti, HMG proteins: dynamic players in gene regulation and differentiation, Curr. Opin. Genet. Dev. 15 (2005) 496–506, https://doi.org/10.1016/j.gde.2005.08.007.
[56] D. Buac, M. Shen, S. Schmitt, F. Rani Kona, R. Deshmukh, Z. Zhang, C. Neslund-Dudas, B. Mitra, Q.P. Dou, From Bortezomib to other inhibitors of the proteasome and beyond, Curr. Pharm. Des. 19 (2013) 4025–4038, https://doi.org/10.2174/1381612811319220012.
[57] C. Liao, R. Beveridge, J.J.R. Hudson, J.D. Parker, S.C. Chiang, S. Ray, M.E. Ashour, I. Sudbery, M.J. Dickman, S.F. El-Khamisy, UCHL3 regulates topoisomerase-induced chromosomal break repair by controlling TDP1 proteostasis, Cell Rep. 23 (2018) 3352–3365, https://doi.org/10.1016/j.celrep.2018.05.033.
[58] T. Kurosaki, L.E. Maquat, Nonsense-mediated mRNA decay in humans at a glance, J. Cell Sci. 129 (2016) 461–467, https://doi.org/10.1242/jcs.181008.
[59] V. Glorian, G. Maillot, S. Polès, J.S. Iacovoni, G. Favre, S. Vagner, HuR-dependent loading of miRNA RISC to the mRNA encoding the Ras-related small GTPase RhoB controls its translation during UV-induced apoptosis, Cell Death Differ. 18 (2011) 1692–1701, https://doi.org/10.1038/cdd.2011.35.
[60] E. London, M. Bloyd, C.A. Stratakis, PKA functions in metabolism and resistance to obesity: lessons from mouse and human studies, J. Endocrinol. 246 (2020) R51–R64, https://doi.org/10.1530/JOE-20-0035.
[61] K.A. Spriggs, M. Bushell, A.E. Willis, Translational regulation of gene expression during conditions of cell stress, Mol. Cell 40 (2010) 228–237, https://doi.org/10.1016/j.molcel.2010.09.028.
[62] S.M.K. Davies, M.I.G. Lopez Sanchez, R. Narsai, A.M.J. Shearwood, M.F.M. Razif, I. D. Small, J. Whelan, O. Rackham, A. Filipovska, MRPS27 is a pentatricopeptide repeat domain protein required for the translation of mitochondrially encoded proteins, FEBS Lett. 586 (2012) 3555–3561, https://doi.org/10.1016/j.febslet.2012.07.043.